

Electromechanical Effects in Carbon Nanotubes

M. Verissimo-Alves¹ * Belita Koiller¹, H. Chacham², and R. B. Capaz¹

¹*Instituto de Física, Universidade Federal do Rio de Janeiro,
Caixa Postal 68528, 21845-970, Rio de Janeiro, RJ, Brazil and*

²*Departamento de Física, ICEEx, Universidade Federal de Minas Gerais,
Caixa Postal 702, 30123-970 Belo Horizonte, MG, Brazil*

(Dated: June 15, 2018)

We perform *ab initio* calculations of charged graphene and single-wall carbon nanotubes (CNTs). A wealth of electromechanical behaviors is obtained: (1) Both nanotubes and graphene expand upon electron injection. (2) Upon hole injection, metallic nanotubes and graphene display a non-monotonic behavior: Upon increasing hole densities, the lattice constant initially contracts, reaches a minimum, and then starts to expand. The hole densities at minimum lattice constants are 0.3 $|e|/\text{atom}$ for graphene and between 0.1 and 0.3 $|e|/\text{atom}$ for the metallic nanotubes studied. (3) Semiconducting CNTs with small diameters ($d \lesssim 20 \text{ \AA}$) always expand upon hole injection; (4) Semiconducting CNTs with large diameters ($d \gtrsim 20 \text{ \AA}$) display a behavior intermediate between those of metallic and large-gap CNTs. (5) The strain versus extra charge displays a linear plus power-law behavior, with characteristic exponents for graphene, metallic, and semiconducting CNTs. All these features are physically understood within a simple tight-binding total-energy model.

PACS numbers: PACS numbers: 71.20.-b, 73.22.-f, 73.90.+f

More than 10 years after their discovery by Iijima [1], carbon nanotubes (CNTs) are still capable of unveiling surprising and fascinating physical properties. An important feature of CNTs is the dependence of their electronic properties on diameter and chirality [2, 3, 4, 5, 6]. However, not only the electronic properties of CNTs are attractive, as these materials have superb mechanical properties as well [7], making their use in nanomechanical applications very promising [8]. The possibility of *electronic* control of nanomechanical devices would certainly bring a great improvement in their effective switching times, control and precision [9].

For all these reasons, it is important to study the electromechanical properties of CNTs. A few experimental works have focused on electrostatically-driven mechanical responses of CNTs [10, 11]. However, mechanical response of CNTs can be driven not only by electrostatics, but also by quantum-mechanical effects. Indeed, it is well known that the in-plane lattice constant of intercalated graphite expands or contracts relative to pure graphite because of charge-transfer effects [12, 13]. Recently, the mechanical response of "nanotube sheets" - sheets of entangled single-wall CNTs bundles - to electrochemical charge injection has been investigated, and its use in actuators has been proposed [14]. In that work, the electromechanical response of CNTs has been found to be stronger and more non-linear than that of graphite. Controlling and optimizing the electromechanical response of nanotube sheets is a difficult task, since it involves problems like bundling and entanglement of CNTs. For these reasons, it would be highly desirable to investigate the electromechanical properties of *individual* nanotubes and their dependence on chirality and diameter. Since experimental control of these parameters is still beyond the current state-of-art, the predictive power of *ab initio*

theoretical calculations makes them the method of choice for such studies.

Initially, we perform *ab initio* calculations of charged graphene and single-wall metallic and semiconducting CNTs. Our calculations are performed within the Density Functional Theory (DFT) and pseudopotential frameworks with a numerical-atomic-orbitals basis set (SIESTA code) [15]. SIESTA has been successfully used in a number of studies on CNTs [16, 17].

Fig. 1(a) shows the relative variation $\frac{\delta L}{L_0}$ of the in-plane lattice parameter for graphene or the unit cell axial length [18] for metallic zig-zag (12,0) and armchair (5,5) CNTs, as a function of the extra charge [19] (in units of $|e|$) per atom, q . Negative q (extra electrons) cause expansion of graphene and metallic CNTs, whereas low positive q (holes) cause contraction. Large amounts of hole injection eventually cause expansion of graphene and CNTs, in qualitative agreement with experiments [14]. Fig. 1(a) also shows, from the comparison between the results for the (5,5) and the (12,0) CNTs, that the electromechanical response of metallic CNTs is sensitive to chirality and/or diameter. Also in agreement with experimental observations, the strain $\frac{\delta L}{L_0}$ vs. q appears to be more non-linear for CNTs than for graphene. The largest negative strain is -0.05% for graphene and -0.06% for (12,0) nanotubes, therefore larger than the experimental value of -0.02 to -0.03%, indicating that the effect of bundling in nanotube sheets may hinder the electromechanical response of CNTs. A linear fit in the $q < 0$ regime for graphene gives $\frac{\delta L}{L_0 q} = 0.060$, in good agreement with the experimental value of 0.066 for intercalated graphite [14].

Fig. 1(b) shows the behavior of $\frac{\delta L}{L_0}$ vs. q for a semiconducting (11,0) CNT. Surprisingly, the CNT expands regardless of the sign of q , in contrast to what is observed

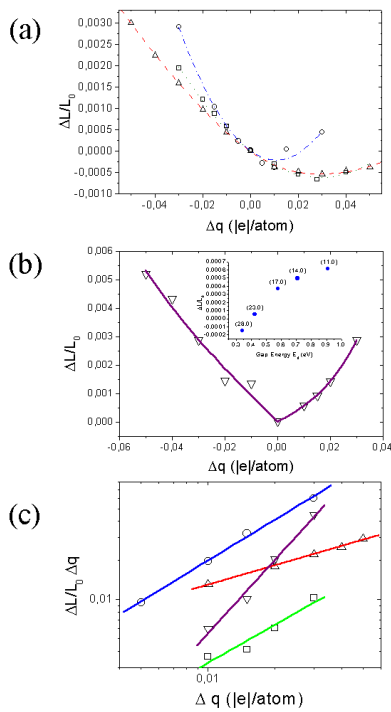


FIG. 1: (a) Relative variation of the lattice constant (for graphene) or the axial unit cell lengths (for metallic CNTs), $\frac{\delta L}{L_0}$, as a function of the extra charge, q . Points are *ab initio* results, lines are best fits using Eqs. (12) and (13). (b) Same as (a) for semiconducting CNTs and fit using Eq. (14). Inset: plot of $\frac{\delta L}{L_0}(q = 0.01)$ for semiconducting CNTs of different diameters, showing the crossover to "metallic-like" behavior. (c) Log-log plots showing the different power laws of $\delta L(q)$, as discussed in the text. The slopes are 0.52 ± 0.04 , 0.94 ± 0.15 , 1.32 ± 0.21 and 1.90 ± 0.15 , for graphene, (12,0), (5,5) and (11,0) CNTs respectively, consistent with the predictions of the TB model (($\alpha - 1$), where α is defined in Eq. (15)): 1/2, 1, 1 and 2.

for graphene and metallic CNTs.

A key element to understand these results is the energy positioning of bonding and anti-bonding states in graphene and CNTs. A widely accepted view, based on a π -orbital, nearest-neighbor (nn) tight-binding (TB) description of the energy bands of graphene [7], is that the lower (valence or π) band has a bonding character and the upper (conduction or π^*) band has an anti-bonding character. Indeed, within such a description, the energy

bands of undistorted graphene are

$$\varepsilon_0(\vec{k}) = \epsilon_{2p} \pm t_0 f(\vec{k}), \quad (1)$$

where ϵ_{2p} is an "atomic level" for the $2p$ state of the C atom (corrected by the crystalline potential), t_0 is the nn hopping integral for an undistorted graphene lattice (lattice constant a_0), and $f(\vec{k})$ is a function of the wave vector in the 2-d Brillouin Zone (BZ) [7]. In this case, ϵ_{2p} coincides with the Fermi level, E_F , for a neutral system at the K points of the BZ, where $f(\vec{k}) = 0$. Therefore, extra electrons would occupy anti-bonding states and extra holes would go to bonding states. In either case the lattice would expand. Therefore, the nn TB approximation cannot explain the contraction of graphene and metallic CNTs for low positive q .

However, as pointed out by Kertesz [23], inclusion of next-nearest-neighbor (nnn) interactions lifts the energy eigenvalues at the K points above ϵ_{2p} , therefore making these states antibonding. Since our method is based on an atomic-orbital basis, we can provide *ab initio* verification of these ideas. From the *ab initio* Hamiltonian (with interactions up to 4th nn), we estimate ϵ_{2p} to be roughly 1.6 eV below E_F for graphene. This is illustrated in Fig. 2. Therefore, the states around E_F are antibonding for both bands, and now if electrons are gradually removed from the π band (positive charging), the bond lengths will contract, in agreement with experiments [14] and with the results in Fig. 1. If positive charging continues, electrons will be eventually removed from states below ϵ_{2p} (therefore from bonding states) and the bond lengths will start to increase again, also in agreement with the *ab initio* results.

We explain this behavior in a more quantitative way via a total-energy TB model. The total energy of graphene or CNTs is a function of the number of electrons per atom, N , and the bond length variation δL , and it is expressed as

$$E_{tot}^N(\delta L) = E_b + E_r = 2 \sum_{\vec{k}}^{occ} \varepsilon_{\delta L}(\vec{k}) + E_r \quad (2)$$

where E_b is the band energy and E_r is a repulsive energy. The summation runs over occupied states (accounting for the proper value of N) and $\varepsilon_{\delta L}(\vec{k})$ is the band structure for a deformation δL .

From Eq. (1), we can write the band structure dependence on the deformation as

$$\varepsilon_{\delta L}(\vec{k}) = \epsilon_{2p} + (\varepsilon_0(\vec{k}) - \epsilon_{2p}) \frac{t_{\delta L}}{t_0}, \quad (3)$$

where $t_{\delta L}$ is the hopping matrix element for a distorted lattice. Assuming a power-law dependence of t on the bond length L , i.e. ($t_{\delta L} = t_0(L_0/L)^\alpha$) and taking the limit of small δL , we can linearize:

$$\varepsilon_{\delta L}(\vec{k}) = \varepsilon_0(\vec{k}) - \zeta \delta L (\varepsilon_0(\vec{k}) - \epsilon_{2p}), \quad (4)$$

where $\zeta = \alpha/L_0$. Let us consider the case of a neutral system, with N_0 electrons. From Eqs. (2) and (4), E_b is given by

$$E_b^{N_0}(\delta L) = E_b^{N_0}(0) - \zeta \delta L [E_b^{N_0}(0) - N_0 \epsilon_{2p}]. \quad (5)$$

For a neutral system, by definition, the total energy must be minimum at $\delta L = 0$, so

$$E_{tot}^{N_0}(\delta L) = E_{tot}^{N_0}(0) + \beta(\delta L)^2, \quad (6)$$

where β is an elastic constant. Substitution of (5) and (6) in (2) yields an expression for the repulsive energy of a neutral system at arbitrary δL :

$$E_r^{N_0}(\delta L) = E_r^{N_0}(0) + \beta(\delta L)^2 + \zeta \delta L (E_b^{N_0}(0) - N_0 \epsilon_{2p}) \quad (7)$$

Consider now a system with an arbitrary number of electrons N . The calculation of E_b is similar to that for the neutral case, yielding

$$E_b^N(\delta L) = E_b^N(0) - \zeta \delta L (E_b^N(0) - N \epsilon_{2p}). \quad (8)$$

We also assume that, to first order, the dependence of E_r on the bond length is not very much affected by the extra charge. Then, from Eq. (7) we have

$$E_r^N(\delta L) = E_r^N(0) + \beta(\delta L)^2 + \zeta \delta L (E_b^N(0) - N \epsilon_{2p}) \quad (9)$$

Combining Eqs. (2), (8) and (9), and defining the extra charge as $q = -\Delta N = N_0 - N$, we finally arrive at an expression for the total energy of a charged system:

$$E_{tot}^q(\delta L) = E_{tot}^q(0) + \beta(\delta L)^2 + \zeta \delta L q (\Delta \tilde{E}_b - \epsilon_{2p}). \quad (10)$$

Here, $\Delta \tilde{E}_b = \frac{E_b^N(0) - E_b^{N_0}(0)}{\Delta N}$ is the variation in band energy per extra electron. By imposing $\frac{\partial E_{tot}^q}{\partial L}|_q = 0$, we obtain the unit cell length distortion as a function of q :

$$\delta L(q) = -\frac{\zeta}{2\beta} q (\Delta \tilde{E}_b - \epsilon_{2p}). \quad (11)$$

Eq. (11) has a very simple physical meaning. Consider for instance electron injection ($q < 0$). If $\Delta \tilde{E}_b - \epsilon_{2p} > 0$, extra electrons are predominantly placed in anti-bonding levels, so the lattice expands ($\delta L > 0$). Similar arguments can be used for electrons in bonding levels (yielding lattice contraction) and holes in anti-bonding or bonding levels (yielding contraction or expansion).

We now calculate $\delta L(q)$ for graphene and CNTs. Let us consider graphene first. In the vicinity of E_F , we can use a simple “conical” approximation for the energy bands, $\varepsilon(\vec{k}) = E_F \pm \gamma |\vec{k}|$, where $+$ stands for electrons and $-$ for holes, and the origin in k -space is shifted to the K point. $\Delta \tilde{E}_b$ may then be obtained by integrating $\varepsilon(\vec{k})$ over the region of the BZ occupied with extra electrons, i.e. a disk of radius Δk which is related to q as $\mp q =$

$\frac{s(\Delta k)^2}{\pi}$, where s is the area per atom. After integrating and substituting the result into Eq. (11), we get

$$\delta L(q) = -\frac{\zeta}{2\beta} q \left[E_F - \epsilon_{2p} \pm \frac{2\gamma}{3} \left(\frac{\pi|q|}{s} \right)^{\frac{1}{2}} \right]. \quad (12)$$

The energy bands of CNTs are obtained by slicing the energy bands of graphene along the proper quantization lines [7]. We show schematically in Fig. 2 the result of this procedure in the vicinity of one of the K points. For metallic CNTs, one of the quantization lines will cross the K point, yielding linear 1-d bands. If the CNT is semiconducting, the 1-d bands will be parabolic.

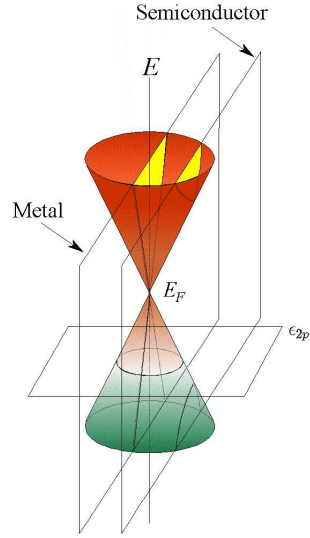


FIG. 2: (color) Schematic band structure of graphene and CNTs, in the vicinity of a K point. The green and red portions of the energy surface indicate bonding and anti-bonding states (energy below and above ϵ_{2p}), respectively. The two vertical planes indicate the effects of k -space quantization for metallic and semiconducting CNTs.

For metallic CNTs, the calculation of $\Delta \tilde{E}_b$ is very similar, the only essential difference being that the integration is now one-dimensional and the integration limits are related to the q as $\mp q = \frac{\Delta k \ell}{\pi}$, where ℓ is the CNT length per atom. The result is

$$\delta L(q) = -\frac{\zeta}{2\beta} q \left(E_F - \epsilon_{2p} - \frac{\gamma \pi q}{2\ell} \right). \quad (13)$$

Finally, for semiconducting CNTs we use a parabolic dispersion $\varepsilon(k) = E_F \pm \frac{\varepsilon_g}{2} \pm \eta k^2$, where ε_g is the energy gap. The result for $\delta L(q)$ is

$$\delta L(q) = -\frac{\zeta}{2\beta} q \left[E_F \pm \frac{\varepsilon_g}{2} - \epsilon_{2p} \pm \frac{\eta \pi^2}{12\ell^2} q^2 \right]. \quad (14)$$

From Eqs. (12), (13) and (14) we see that the electromechanical behaviors of graphene and CNTs can all

be described by simple expressions:

$$\frac{\delta L(q)}{L_0} = -aq + b|q|^\alpha, \quad (15)$$

where the linear coefficient a controls the electromechanical response for low charge injection and depends precisely on the positioning of E_F with respect to ϵ_{2p} . The non-linear term is defined by the exponent α , which is 3/2, 2 and 3 for graphene, metallic and semiconducting CNTs. We test these predictions from the *ab initio* results. In Fig. 1(c) we display log-log plots of $\frac{\delta L}{L_0 q} + a$ vs. $|q|$ for each system. Within error bars, the exponents predicted by the simple TB model are beautifully confirmed by the *ab initio* results. Notice that both (5,5) and (12,0) metallic CNTs have the same exponent $\alpha = 2$. The stronger non-linearity in strain vs. q for the (5,5) CNT - evident from Fig. 1(a) - is due to a higher coefficient of the quadratic term in $\frac{\delta L}{L_0}(q)$. Such a large difference in the quadratic term indicates a strong dependence of the non-linear response of metallic CNTs on their chirality.

Let us consider again semiconducting CNTs. From Fig. 2 and Eq. (14), we see that, for large enough ϵ_g , the upper valence states will stay below ϵ_{2p} . Therefore, for positive q , electrons will be removed from bonding states and expansion will occur. This is precisely what Fig. 1(b) shows. On the other hand, we can predict that if ϵ_g is small enough, semiconducting CNTs will behave qualitatively like metallic ones, i.e., contracting upon hole injection. Since, $\epsilon_g \propto 1/d^2$ (where d is the CNT diameter) [7], we test this prediction by performing *ab initio* calculations on zig-zag semiconducting CNTs of different diameters. The inset of Fig. 1(b) shows a plot of $\delta L/L_0$ as a function of d for a fixed, small extra charge of 0.01 holes/atom. This indeed shows that the decrease in the gap of (n,0) semiconducting CNTs with increasing n ultimately leads to a recovery of metallic nanotube behavior.

In conclusion, we have performed *ab initio* studies of electromechanical effects in graphene and CNTs. The diversity on electromechanical responses is fascinating, and it has an amazingly simple explanation in terms of the bonding and anti-bonding nature of the electronic states within a TB model. The observed stronger non-linear behavior in $\delta L(q)$ for CNTs as compared to graphene is reproduced and explained, arising naturally as a dimensionality effect in the distribution of extra electrons over the BZ's of graphene and CNTs. Our results provide important guidelines for fabrication of nanoelectromechanical devices. Indeed, when experimental control of production and assembling of nanotubes with specific chiralities is achieved, the possibilities in the architecture of different devices by combining the variety of effects described here will be only limited by our imagination.

This work was partially supported by Brazilian agencies CAPES, CNPq, FUJB, FAPERJ, PRONEX-MCT

and Instituto do Milênio de Nanociências. We wish to thank Maurício Araújo for help with preparation of Fig. 2.

Note added: After the submission of this work, a related study by Gartstein *et al* [24] has appeared in the literature.

* Electronic address: verissim@if.ufrj.br

- [1] S. Iijima, *Nature* **354**, 56 (1991).
- [2] N. Hamada *et al.*, *Phys. Rev. Lett.* **68**, 1579 (1992).
- [3] R. Saito *et al.*, *Appl. Phys. Lett.* **60**, 2204 (1992).
- [4] J. W. G. Wildöer *et al.*, *Nature* **391**, 59 (1998).
- [5] Z. Yao *et al.*, *Nature* **402**, 273 (1999).
- [6] S. J. Tans *et al.*, *Nature* **393**, 49 (1998).
- [7] R. Saito, G. Dresselhaus and M. S. Dresselhaus, *Physical Properties of Carbon Nanotubes*, Imperial College Press, 1998.
- [8] J. Cumings and A. Zettl, *Science* **289**, 602 (2000).
- [9] L. Forro, *Science* **289**, 560 (2000).
- [10] P. Poncharal *et al.*, *Science* **283**, 1513 (1999).
- [11] P. Kim and C. M. Lieber, *Science* **286**, 2148 (1999).
- [12] M. S. Dresselhaus and G. Dresselhaus, *Adv. Phys.* **30**, 139 (1980).
- [13] *Proceedings of the 8th International Symposium on Intercalation Compounds*, edited by J. E. Fischer *et al.*, *J. Phys. Chem. Solids* **57**, Nos. 6-8 (1996).
- [14] R. H. Baughman *et al.*, *Science* **284**, 1340 (1999).
- [15] D. Sánchez-Portal *et al.*, *Int. J. Quantum Chem.* **65**, 453 (1997); P. Ordejón *et al.*, *Phys. Rev. B* **53**, R10441 (1996). We use soft pseudopotentials [20] and the generalized gradient approximation [21]. 1326 points are used for sampling the 2-d BZ of graphene, and 13 points for sampling the 1-d BZ of the CNTs, using the scheme of Monkhorst and Pack [22]. A double- ζ basis is used. Hexagonal supercells with in-plane parameter of 30 Å are used to separate periodic images. Forces are converged to less than 10 meV/Å. As usual in supercell schemes, a "jellium" with opposite extra charge ensures system neutrality as a whole.
- [16] M. Veríssimo-Alves *et al.*, *Phys. Rev. Lett.* **86**, 3372 (2001).
- [17] S. Reich *et al.*, *Phys. Rev. B* **64**, 195416 (2001); D. Sánchez-Portal *et al.*, *Phys. Rev. B* **59**, 12678 (1999); M. S. C. Mazzoni and H. Chacham, *Phys. Rev. B* **61**, 7312 (2000); Y. G. Yoon *et al.*, *Phys. Rev. Lett.* **86**, 688 (2001).
- [18] Our calculations include full axial and radial relaxation induced by charge injection. We show here only the axial changes, which are the most relevant ones for possible applications of these electromechanical effects. Anisotropies between radial and axial behavior, as previously obtained [16], are also present here.
- [19] We consider a range of injected charge $-0.05 < q < 0.05$, well within the reported experimental values for graphite intercalated compounds [14]. Those can be taken as estimated bounds for charge injection in CNTs.
- [20] N. Troullier and J. L. Martins, *Phys. Rev. B* **43**, 2006 (1991).
- [21] J. P. Perdew *et al.*, *Phys. Rev. Lett.* **77**, 3865 (1996).
- [22] H. J. Monkhorst and J. D. Pack, *Phys. Rev. B* **13**, 5188

(1976).

[23] M. Kertesz *et al.*, Mat. Res. Soc. Symp. Proc. **20**, 141 (1983).

[24] Yu. N. Gartstein *et al.*, Phys. Rev. Lett. **89**, 045503 (2002).